Impact of Holocene relative sea-level changes on patch reef-island development in the Spermonde Archipelago, South Sulawesi, Indonesia

Michael G Hynes,[1,2] iD **Halwi Masdar,[3] Dedi Parenden,[4]** iD
Nicole J de Voogd,[1,5] iD **Jan-Berend W Stuut,[6,7] Jamaluddin Jompa,[3]**
Jody M Webster[8] and Willem Renema[1,2]

Abstract

Reef cores that have been radiometrically dated are increasingly used to examine Holocene reef geomorphology, accretion rates, and community changes. Further, these accretion rates can be compared to sea level change regimes to see if, and how coral reefs have been keeping up with sea level. As Sea level rise is expected to accelerate over the next 100 years, it is important to examine whether these reef complexes are able to "keep up" and avoid "drowning." Coring has been conducted in many highly studied areas such as the Great Barrier Reef and the Caribbean. However, in the Indo-Pacific region, an area of the highest coral diversity, there have been only a handful of reef cores collected. Here, we present data of 16 cores from two islands of different reef zones from the Spermonde Archipelago, South Sulawesi, Indonesia. Cores were taken from the reef flat and slope, with recovered length varying from 0.41 to 3.53 m, providing a history of each reef after radiocarbon dating. From 7200 to 5500 YBP, sea level rise rapidly increased and these reef complexes accreted at rates able to match this. This is in part driven by a higher occurrence of massive and foliose corals. After this point and toward the present day, sea level declined, causing sub-aerial exposure of these sand cays and the slope now sustaining the growth. This shows that these reef complexes (some of which contain heavily populated islands) are able to keep growing in the face of sea level rise regimes.

Keywords

accretion, carbonate production, coral triangle, geomorphology, progradation, reef cores

Received 25 September 2024; revised manuscript accepted 18 December 2024

Introduction

Tropical coral reefs are unique ecosystems with a high concentration of biodiversity that provide numerous ecological and economic benefits for animals and humans alike (Hoegh-Guldberg et al., 2019). For tropical coastal communities, reefs function as protection, a natural and self-regenerating break from waves and storms (Kench et al., 2022). Further, as reefs accrete and erode, they provide a source of sediment and framework for low lying islands to develop and maintain sub aerial exposure (Kench and Mann, 2017; Montaggioni et al., 2021). Besides the geomorphological processes, reefs also act as a valuable socioeconomic resource for both the fishing and tourist industries in the tropics (Bejarano et al., 2019; Teichberg et al., 2018). The reef functions are maintained, in part, by the complex 3-dimensional structures that reef building corals provide as habitat for other species such as reef fish.

One of the key functions that drives reef growth and resilience, is vertical reef accretion (Gischler and Hudson, 2019; Kench et al., 2022; Morgan et al., 2020), which allows for a sustained buildup of carbonate habitats for countless organisms in the face of sea level rise, bio erosion, and other stressors. This is done by carbonate producers, driven largely by scleractinian corals, but also by foraminifera, mollusks, and calcareous algae (both red and green) (Gischler and Hudson, 2019; Januchowski-Hartley

et al., 2017; Ryan et al., 2019). Further, sediment input from terrestrial sources, as well as biogenic silica can add to a reef's net

[1]Naturalis Biodiversity Center, The Netherlands
[2]Institute for Biodiversity and Ecosystem Dynamics (IBED), Universiteit van Amsterdam, The Netherlands
[3]Marine Science Department, Faculty of Marine Science and Fisheries, Universitas Hasanuddin, Indonesia
[4]Department of Fisheries, Faculty of Fisheries and Marine Science, Universitas Papua, Indonesia
[5]Institute of Biology, Leiden University, The Netherlands
[6]Department of Ocean Systems, NIOZ Royal Netherlands Institute for Sea Research, The Netherlands
[7]Faculty of Science, Department of Earth Sciences, Vrij Universiteit, The Netherlands
[8]Geocoastal Research Group, School of Geosciences, The University of Sydney, Australia

Corresponding authors:
Michael G Hynes, Naturalis Biodiversity Center, PO Box 9517, Leiden 2300 RA, The Netherlands.
Email: mike.hynes@naturalis.nl

Willem Renema, Naturalis Biodiversity Center, PO Box 9517, Leiden 2300 RA, The Netherlands.
Email: willem.renema@naturalis.nl

accumulation (Łukowiak et al., 2018). Accretion rates are impacted by several factors including water depth and therefore light availability and accommodation space (the space available for coral driven sediment accumulation) (Hubbard, 2009; Hubbard et al., 1986). As an increase in water depth increases accommodation space, sea level rise is a major extrinsic factor impacting net vertical accretion (Gischler, 2008; Morgan et al., 2020). Reefs must accrete at rates fast enough to keep water depth at an ideal limit, ensuring that they still receive the optimal amount of light. This leads to a "catch-up" or "keep-up" scenario where reefs are either forced to accrete faster (catch-up) or to maintain their current pace (keep-up) of accretion. If they are unable to do either, then the water depth above becomes too great and they risk becoming a "drowned" reef (Hubbard, 2009). Accretion rates varied across the Holocene, but on average reefs accreted in the 3–10 mm/yr range (Gischler and Hudson, 2019; Hynes et al., 2024; Morgan et al., 2016), which was sufficient to ensure continued accretion in the face of sea level rise. As reefs in the present and into the future are facing unprecedented levels of coral cover loss due to changing climate regimes and direct human impact (through pollution and overfishing), this may result in negative impacts to the broader ecological services that they provide. It is therefore vital to understand how reefs have been able to overcome environmental pressures in the past, and how reef accumulation was able to continue a net positive accretion rate (Morgan et al., 2020; Perry et al., 2015, 2020; Ryan et al., 2019).

Reef growth can be quantified by either measuring the carbonate production or sediment capture side of reef accumulation. Carbonate budgets are a well-calibrated tool used to measure a reef's net carbonate production at a locality (Januchowski-Hartley et al., 2017; Lange et al., 2020). However, this requires a thorough knowledge of several local factors, such as coral coverage and associated accumulation rates, bioerosion, and specific coral growth rate measurements (Lange et al., 2020; Perry et al., 2013, 2020). Further, these carbonate budgets only measure net production at the locality, and do not account for sediment transport into or out of the system. Alternatively, reef cores, in conjunction with radiometric dating, are a unique and well-studied tool for examining variations in vertical reef accretion (from the capture side) across the Holocene (Cramer et al., 2017; Gischler and Hudson, 2019; Hammerman et al., 2022; Hynes et al., 2024; Morgan et al., 2016; Łukowiak et al., 2018). Such studies build knowledge of past reef accretion at many local, and sometimes even regional, scales. Understanding how a reef has grown in the past under varying climatic scenarios helps us to understand current and future accretionary patterns (Dechnik et al., 2019; Gischler and Hudson, 2019; Morgan et al., 2020; Perry and Smithers, 2011; Toth et al., 2015). The large majority of the cores used in previous studies were taken from well-studied reef systems in the Caribbean and the Australian Great Barrier Reef, lesser so islands in the Pacific and Indian Ocean, and to an even lesser extent, Japanese islands make up most of the cores for the Coastal West Pacific Region (Hynes et al., 2024). Noteworthy is the lack of Holocene reef data from reef cores in the region with the highest coral reef diversity and harboring 30% of the world's coral reefs, namely the Coral Triangle.

The Coral Triangle is an area of convergence of high biodiversity and speciation, holding over 600 species of scleractinian corals, and is delineated from central and east Indonesia in the West, to Papua New Guinea in the East, and the Philippines in the North (Hoeksema, 2007; Lane and Hoeksema, 2016; Renema et al., 2008). Despite this area long being known as a harbor of tropical diversity, most research only goes back decades and only three Holocene core studies are known from the area, one from Bohol in the Philippines (Grobe et al., 1985) and two more recently from Sulawesi, Indonesia (Kappelmann et al., 2023, 2024). These two other core studies from Spermonde are focused on cores from the islands themselves, and have not investigated the geomorphological history of the reef flat or slope (which make up a large portion of the patch reef complex). Hence, there is little insight into past reef accumulation rates and their relation to environmental conditions in the area, which in turn hinders the ability to predict whether reefs in the Coral Triangle are able to accrete at rates fast enough to keep up with changing environmental conditions, including under future sea level rise scenarios (Morgan et al., 2020). This increase in sea level will especially have an impact on low lying islands, such as those populated throughout the Indo-Pacific regions, which face an increased risk of flooding, or disappearing altogether. Coupled with overfishing and other destructive fishing practices, communities who rely on these reefs could be facing extreme uncertainty for their future (Ballesteros et al., 2018; Bejarano et al., 2019; Teichberg et al., 2018). Furthermore, other more intensively studied regions all have their own varying accretion regimes, and major influencing factors cannot be directly applied from one locality/region to the next. With the knowledge gained from these Holocene reefs, we can apply this to studying the context of current and future reef accumulation within the Coral Triangle.

To better understand how reef complexes (some with sand cays) in the Coral Triangle formed and continued to grow throughout the Holocene, we collected and examined a suite of reef matrix cores from two islands in the Spermonde Archipelago, South Sulawesi, Indonesia. The geomorphological evoultion and accumulation history captured within these cores will allow for an understanding of how these reefs fared under different sea level and climate scenarios during the Holocene. Sedimentary facies, grain size analysis, and other geologic data was collected from these cores. Radiometric dates have been obtained from all cores to determine the timing of these events on the reefs. The Early to Mid-Holocene is a period where significant sea level rise occurred, and during this time low-lying island platforms began to form and accrete. In turn, we can then use this knowledge of reef accretion and formation in the area to better predict how they might respond under present, and potentially even future scenarios. It is especially important and relevant for local populations living in low lying islands and coastal areas to understand how these islands will fare under future sea level rise, as the rate of sea level rise has already doubled in the last 30 years (Walker et al., 2021) and IPCC estimates for the region under an RPC4.5 (moderate emissions scenario) that sea level could be rising by a rate of 5.5 mm/yr over the next 100 years.

Materials and methods

Location and setting

The Spermonde Archipelago, located in Southwest Sulawesi, Indonesia, is a series of some 120 coral islands along a carbonate shelf (Figure 1). Approximately 80 of these islands see continuous sub-aerial exposure (Yusuf et al., 2021). The coral islands are patch reefs that developed on zonated ridges running roughly parallel in a North-South direction, with a patchy barrier reef separating it from the Makassar strait (Janßen et al., 2017; Kench and Mann, 2017). The location of these islands is determined by underlying karst pillars from the Eocene to Miocene Tonas limestone, likely topped by older Pleistocene reefs. The islands tend to follow a general composition pattern - The reef patch complex has a crest (and sometimes an accompanying rampart) at or above sea level on the seaward (Western) rim, which protects a shallow reef flat and accompanying island. The reef flat currently has relatively low coral cover, decreasing in area coverage as you move toward the island itself. On the leeward (Eastern) edge, there is now a less pronounced crest, and the platform slopes off gently to reef base. Outside of the crest on the seaward side is a reef slope where the majority of coral cover and diversity is contained (Girard et al., 2022; Renema and Troelstra, 2001). Here we see approximately 70 genera and over 225 species of coral (Best et al., 1989; Moll, 1983; Veron, 1995, 2000). The most common genera are *Acropora*, *Montipora*, *Seriatopora*, *Porites*,
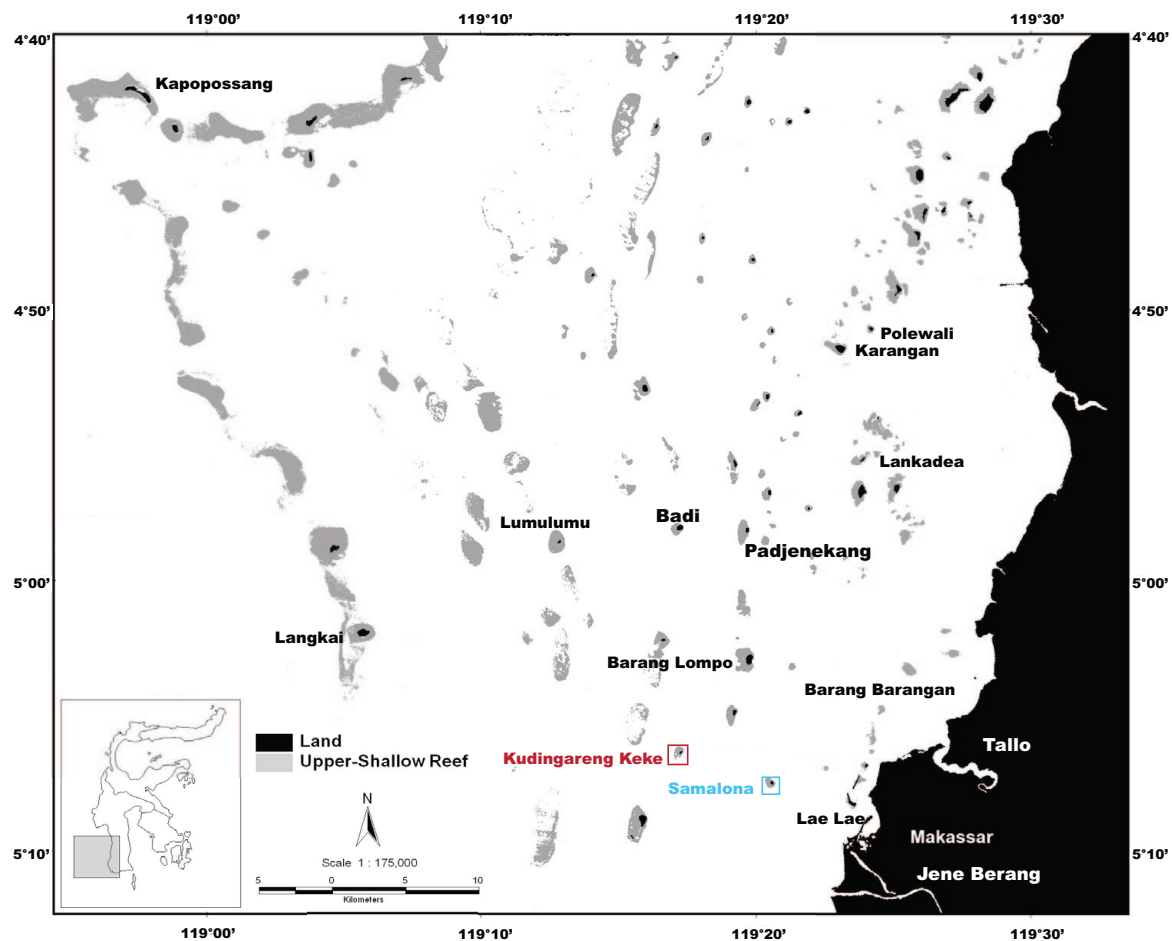
Figure 1. Map of the Spermonde Archipelago adapted from (Plass-Johnson et al., 2016; van der Windt et al., 2020). Blue shows the island Samlaona, red the island Kudingareng Keke.
Note. Please refer to the online version of the article to view this figure in color.

Pocillopora, as well as the family Fungiidae (Moll, 1983; Moll and Borel-Best, 1984). Between islands, the inter-reef is sandy bottomed, with water depth increasing up to approximately 70 m.

Adjacent to the archipelago is the large city of Makassar (over 1.5 million people) which sits between three river mouths, the Jene Barang to the south, and the Tallo and Maros rivers North of the city. There are also several smaller tributaries to the north. This influences the entire shelf system via the introduction of nutrients and sediments from the city and rivers onto the reef islands. This influential turbidity regime sees a gradient of high turbidity near the shoreline, with decreasing turbidity moving toward the outer barrier islands. Further, almost half of these islands are inhabited with a dense population covering nearly the entire surface of the island, and anthropogenic structures (such as jetties and breakwaters) being built onto the reef, impacting the ecosystem's development. Biologically, the Spermonde archipelago is at the center of The Coral Triangle (hereafter referred to CT) and therefore is one of the most diverse reef systems in the world (Hoeksema, 2007; Moll, 1983; Moll and Borel-Best, 1984). However, from in-depth and long-term studies conducted on the area, a decline in coral diversity and coral cover of over 30% has been identified in the region since the 1980s (Best et al., 1989; Moll, 1983; Yasir Haya and Fujii, 2017).

Two of these islands, Samalona and Kudingareng Keke, are close to Makassar in the Mid-Shelf Zone, and the closest part of the Outer Shelf Zone respectively. There is a size difference between these two islands, with Samalona island having an approximate area of 2.2–2.8 ha, whereas Kudingareng Keke is only 1.3–1.6 ha (Kench and Mann, 2017). This difference in size is also accompanied by a difference in shape, with Samalona being more rounded and stable, whilst Kudingareng Keke is a narrow cay. Kudingareng Keke has a deposition bar/beach on the North side of the island that is subject seasonal shifts in beach shape and position due to seasonal changes of wind/wave directions (de Klerk, 1983; Kench and Mann, 2017). Wind, wave, and current energy is directed from the Southeast during the monsoon season which impacts the formation of these islands. However, during the dry season, the dominant energy direction is from the Northwest, but with a much lower magnitude of energy. This same dynamic on the northern shore is also seen on Samalona (de Klerk, 1983), but is less conspicuous due to Samalona's size, and its high level of vegetation. Interestingly, this vegetation was largely planted by humans in the beginning of the previous century. The total reef area is slightly larger on Kudingareng Keke at 55.8 ha, versus Samalona reef which is only 40.3 ha. Samalona is populated, and was and has been a tourist spot where locals and visitors come to snorkel, dive, and use the island for other forms of activity. Kudingareng Keke has never been permanently inhabited, although a tourist resort was planned to be built there in the 1990s, and it is used as an overnight stay for fishers. In the past decades, a similar style of day tourism as on Samalona has developed. Further, a viewing tower has since been built on the island. Both islands are seeing more frequent use for tourism, and therefore are experiencing an increased impact of anthropogenic activities.

Core collection

We collected 16 Reef Sediment/Framework Cores from two islands (Samalona and Kudingareng Keke, Figures 1–3) in August 2022 using open barrel push coring techniques (Cramer et al., 2017;
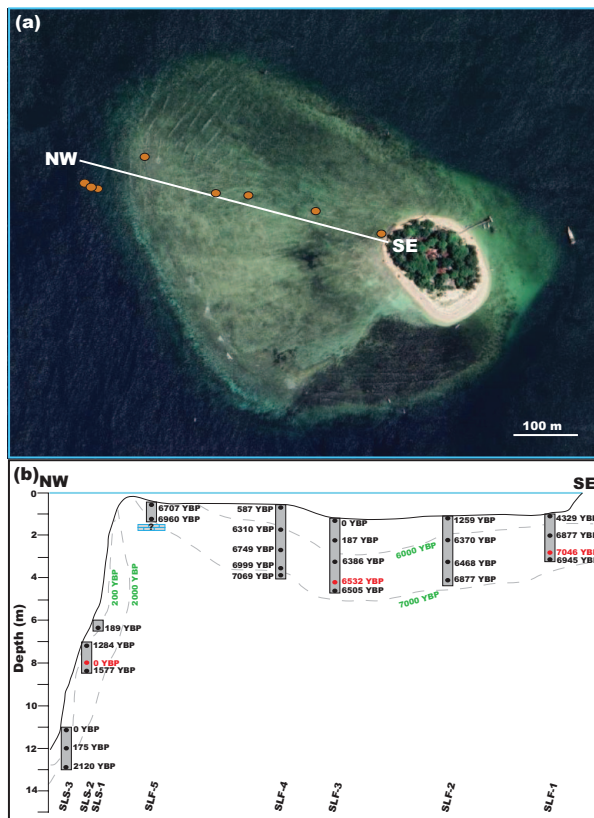
Figure 2. (a) Core transect of Samalona on the island platform (Satellite image Bing 2024). (b) Cross section of coring transect from Samalona. Black dates are calYBP ^{14}C dates. Red dates/* are calYBP ^{14}C dates representing an age reversal. Green dates/dashed lines are geomorphological isochrons. Core names are at the bottom.
Note. Please refer to the online version of the article to view this figure in color.

Figure 3. (a) Core transect of Kudingareng Keke on the island platform (Satellite image Bing 2024). (b) Cross section of coring transect from Kudingareng Keke. Black dates are calYBP ^{14}C dates. Red dates/* are calYBP ^{14}C dates representing an age reversal. Green dates/dashed lines are geomorphological isochrons. Core names are at the bottom.
Note. Please refer to the online version of the article to view this figure in color.

Macintyre and Glynn, 1976; Perry and Smithers, 2010; Łukowiak et al., 2018). Six meter-long aluminum tubes with an external diameter of 75 mm and internal diameter of 69 mm were hammered into the reef with a slide hammer. This was done both at the water level on the reef flat, and by aid of SCUBA for the reef slope. Reef slope cores were placed on rubble patches near living coral colonies to avoid harming live coral. Water depth of each core was measured relative to Mean Sea Level (MSL) as calculated previously (Bender et al., 2020; Mann et al., 2016). Cores were taken along an approximate SE-NW transect to follow the island platform shape. From Samalona, five cores were collected on the reef flat (Core Names SLF-[1-5], see Table 1), and three from the reef slope (SLS-[1-3], Table 1), whilst on Kudingareng Keke one core was collected from the island (KKI-1), four from the flat (KKF-[1-4], Table 1) and another three on the reef slope (KKS-[1-3], Table 1). The coring tube was hammered in until it no longer was able to penetrate, usually accompanied by a feeling of hitting hard carbonate.

Cores were first logged and photographed for sedimentology and stratigraphy following standard sedimentological procedures (Boggs, 2012). They were then broken down into 5 cm subsamples, a common practice for reef cores (Cramer et al., 2017; Palmer et al., 2010; Perry et al., 2011), which helps compensate for compaction, mixing, bioturbation, and time averaging (Kidwell, 1997, 2013). The subsamples were vacuum packed using a food sealer and shipped to Naturalis Biodiversity Center in the Netherlands for further research. The subsamples were sieved into two size fractions (larger and smaller than 2 mm) using standard geological techniques. Sieving was conducted by rinsing with fresh water to remove any salt on the sediments. The >2 mm fraction (pebbles and larger) includes the majority of coral pieces, as well as other carbonate producing organisms
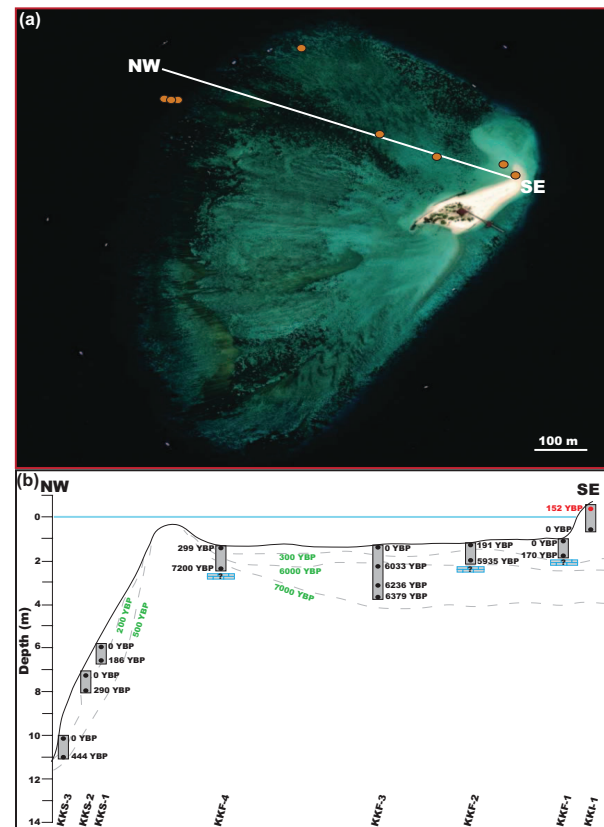
(such as mollusks, algae), while the <2 mm fraction (sand and smaller grains) is mostly eroded carbonate matrix material as well as smaller carbonate producers, such as foraminifera, and siliceous sponge spicules. Sieved fractions were then placed in an oven at 55°C for 24–48 h until fully dry.

Radiometric dating

To determine the geochronological framework along the island platform, we conducted radiocarbon (^{14}C) dating on mollusk shells from the cores (Table 2). Carbonate shells were collected from the >2 mm fraction approximately every 1 m downcore. Only shells with enough carbonate material and without visible diagenesis, no external encrusting carbonate organisms, and minimal erosion were used. We chose mollusk shells over in situ corals, as the mollusk shells had much better preservation than the corals, especially for the oldest samples and are easier to determine if there is any allochthonous carbonate (Woodroffe et al., 2007). Shells were cleaned by hand using paintbrushes and dental picks, soaked in Deionized (DI) water, dried at 55°C overnight, then placed into a sonic bath of DI water for 15 min. Samples were then shipped to DirectAMS, an isotope lab in Washington State, where they were acid-etched and placed into an Accelerator Mass Spectrometer (AMS) to obtain conventional radiocarbon dates reported in years before present (YBP). Conventional ^{14}C dates were calibrated using CALIB version 8.2.0 using the Marine20 curve (Heaton et al., 2020; Stuiver et al., 2022; Stuiver and Reimer, 1993) to correct for the marine reservoir effect and then reported in calYBP. As there was no exact local reservoir correction value (ΔR), we averaged the 10 nearest points from the

Table 1. Metadata for each reef core collected and described within this study.

Core ID	Date collected	Island	Water depth (m)	Latitude	Longitude	Reef locale	Penetration (m)	Recovery (m)	Compaction %
KKI-1	19/08/2022	Kudingareng Keke	−1	−5.104895	119.289417	Island	2.5	1.14	45.6
KKF-1	14/08/2022	Kudingareng Keke	1	−5.104706	119.289257	Flat	1.1	0.71	64.55
KKF-2	14/08/2022	Kudingareng Keke	1.3	−5.104581	119.288322	Flat	1	0.85	85
KKF-3	14/08/2022	Kudingareng Keke	1.2	−5.104136	119.287517	Flat	3.7	2.56	69.19
KKF-4	19/08/2022	Kudingareng Keke	1.4	−5.102445	119.28644	Flat	3.6	1.1	30.56
KKS-1	16/08/2022	Kudingareng Keke	9.9	−5.103428	119.284535	Slope	2.5	1.11	44.4
KKS-2	16/08/2022	Kudingareng Keke	7.2	−5.103438	119.284588	Slope	1.65	0.89	53.94
KKS-3	16/08/2022	Kudingareng Keke	6	−5.103375	119.284689	Slope	1.55	0.78	50.32
SLF-1	15/08/2022	Samalona	1	−5.124956	119.34266	Flat	3.95	2.27	57.47
SLF-2	15/08/2022	Samalona	1	−5.124597	119.341783	Flat	4.55	3.17	69.67
SLF-3	21/08/2022	Samalona	1.2	−5.124336	119.340864	Flat	5	3.53	70.6
SLF-4	21/08/2022	Samalona	0.5	−5.124303	119.34041	Flat	5.1	3.46	67.84
SLF-5	21/08/2022	Samalona	0.4	−5.12372	119.339448	Flat	1.2	0.89	74.17
SLS-1	18/08/2022	Samalona	11.1	−5.12413	119.338657	Slope	3.9	2.1	53.85
SLS-2	18/08/2022	Samalona	7.1	−5.124216	119.338735	Slope	2.5	1.46	58.4
SLS-3	18/08/2022	Samalona	6.6	−5.124231	119.338772	Slope	1	0.41	41

Marine20 Reservoir Database ($\Delta R = −254 \pm 151$) and used this to correct the marine reservoir effect.

Calculation of accretion rates

Mean Accretion Rates (hereafter called MAR) were calculated as previously described in the RADReef database (Hynes et al., 2024). This requires a minimum of two dates per core as it determines the difference between depths (D) divided by the difference in ages (t) using the following formula: $MAR = (D_2 − D_1) / (t_2 − t_1)$. Age reversals were removed prior to calculating MAR, as this would create a negative accretion rate value. Mean Time (hereafter Mt) for each MAR were calculated by averaging the two dated points used for a MAR calculation (t_1 and t_2). Paleo Reef Depth (hereafter PRD) was calculated by adding the core depth of a dated sample to its water depth relative to Mean Sea Level. This was done to aid in more direct comparisons of samples from within and external to this study.

Grain size analysis of sediments

Grain size analysis was conducted on the <2 mm fraction to determine if reef sediment infill has changed through the Holocene. A few grams of sediment were collected approximately every 25 cm downcore. These were added to a Beckman Coulter Laser Diffraction Particle Size Analyzer (0.04–2000 μm size range) with an Aqueous Liquid Module (LS 13 320) until obscurity was between 8% and 12% then run multiple times until the grain size curve stabilized. These multiple runs were done to account for clumped sediment as well as air bubbles that may have entered the laser scanner from the Reverse Osmosis water system. The final run of each sample was then used for comparison. This was done to determine the distribution of sand, silt, and clay particles for each subsample.

Sea level curve

To examine the effect of sea level on accretion rates and island geomorphology, we generated a regional Relative Sea Level (RSL) curve for the Coastal West Pacific. These were generated by using RSL and accompanying calibrated ^{14}C dates previously calculated (Lambeck et al., 2014). Dates were already calibrated within the study for uniformity and were therefore not recalibrated here. The Paleo Sea Level Region examined here, Coastal West Pacific, was created using data points previously collected to determine sea level regions (Khan et al., 2019). The RSL curve

was generated using R package ggplot2 to create a loess regression with a 95% confidence interval (Wickham, 2016).

Results

Cores

Recovered lengths of the cores varied between 0.41 and 3.53 m (average of 1.61 m, SD 1.03) where post compaction recovery % (recovery/penetration × 100) ranged from 30.6% to 85%, with an average of 58.3% (Figures 2 and 3, Table 1). The low average recovery percentage is likely due to compaction from percussion coring, as well as some incidental material loss from the bottom of the cores during core retrieval. The longest cores were all collected from the reef flat and the average length of recovery was almost 1 m longer than on the slope (2.06 m, SD 1.18 flat, vs 1.13 m, SD 0.59 slope). We collected three reef flat cores with a recovered length of over 3 m from Samalona, and only one from Kudingareng Keke. Furthermore, on Samalona we collected one reef slope core of over 2 m recovered length. Average recovery percentage on Samalona was slightly higher (61.6%) compared to Kudingareng Keke (55.4%), but both are comparable to the total average recovery value. On the flat of Kudingareng Keke, three out of four cores hit an impenetrable carbonate surface (where coring could no longer continue, and the coring pipe had a metallic ring due to hitting solid carbonate) which terminated coring, whereas on Samalona this only occurred once on the flat.

Core lithologies/facies

Facies were determined by combination of the most dominant coral morphology (branching, foliose, or massive), as well as by determining if they were rudstone (the >2 mm fraction is more than 50% of the subsample) or floatstone (the >2 mm fraction is less than 50% of the sub sample). Rudstone was used for the clast supported facies as the clasts were in contact with each other. This was done as we could not definitively say that all of the >2 mm components were in situ, even though they all were produced locally within the same patch reef system. Within all cores collected here, six different facies were identified. Figure 4a represents the branching-dominant rudstone facies, where there are large and numerous pieces of branching framework supporting the infilled matrix. The branching floatstone facies (Figure 4b), again sees branching corals dominant, but with the infilled sediment matrix being the majority of the core. A massive dominant rudstone facies (Figure 4c) has a majority of massive coral pieces,

Table 2. 14C radiometric dating data from all 45 samples taken. This includes the raw and calibrated data, as well as the MAR, mean age, and PRD results.

| Core	Organism class	Lab code	Section (cm)	Mean depth (cm)	pMC (% modern Carbon)	Error	Uncalibrated age (YBP)	1σ Error	ΔR	Uncertainty	Min 1σ	Max 1σ	Min 2σ	Max 2σ	Mean probability age	Paleo reef depth (mm)	MAR (mm/yr)	Mean age (YBP)	Age reversal
SLF-1	Gastropod	D-AMS 050631	(5–10)	7.5	59.85	0.18	4124	24	−254	151	4101	4535	3917	4773	4329	1075			N
SLF-1	Gastropod	D-AMS 050632	(130–135)	132.5	45.43	0.19	6338	34	−254	151	6683	7068	6502	7241	6877	2325	0.490581	5603	N
SLF-1	Gastropod	D-AMS 050633	(200–205)	202.5	44.55	0.18	6495	32	−254	151	6875	7238	6685	7393	7046	3025	13.23529	6911	Y
SLF-1	Gastropod	D-AMS 050634	(220–227)	222.5	45.08	0.12	6400	21	−254	151	6772	7143	6577	7297	6945	3225			N
SLF-2	Gastropod	D-AMS 050635	(10–15)	12.5	81.85	0.21	1609	21	−254	151	1072	1418	916	1606	1259	1125			N
SLF-2	Bivalve	D-AMS 050636	(110–115)	112.5	48.11	0.15	5878	25	−254	151	6192	6549	5997	6727	6370	2125	0.195656	3814.5	N
SLF-2	Gastropod	D-AMS 050637	(202–207)	204.5	47.56	0.16	5970	27	−254	151	6287	6640	6114	6844	6469	3045	9.292929	6419.5	N
SLF-2	Gastropod	D-AMS 050638	(312–317)	314.5	45.43	0.16	6338	28	−254	151	6685	7067	6505	7240	6877	4145	2.696078	6673	N
SLF-3	Gastropod	D-AMS 050639	(10–15)	12.5	100.64	0.23	0	0	−254	151					Modern	1325			N
SLF-3	Gastropod	D-AMS 050640	(105–110)	107.5	94.69	0.26	438	22	−254	151	30	257	1	429	187	2275	5.080214	93.5	N
SLF-3	Gastropod	D-AMS 050641	(209–214)	211.5	48.02	0.17	5893	28	−254	151	6204	6562	6007	6741	6386	3315	0.167769	3286.5	N
SLF-3	Gastropod	D-AMS 050642	(304–309)	306.5	47.21	0.16	6029	27	−254	151	6342	6705	6185	6906	6532	4265			Y
SLF-3	Gastropod	D-AMS 050643	(339–344)	321.5	47.36	0.15	6004	25	−254	151	6310	6668	6163	6886	6505	4415	9.243697	6445.5	N
SLF-4	Gastropod	D-AMS 050644	(15–20)	17.5	89.25	0.22	914	20	−254	151	444	729	295	894	587	675			N
SLF-4	Bivalve	D-AMS 050645	(100–105)	102.5	48.44	0.15	5823	25	−254	151	6125	6489	6391	7136	6310	1525	0.148524	3448.5	N
SLF-4	Bivalve	D-AMS 050646	(202–207)	204.5	46.08	0.14	6224	24	−254	151	6555	6938	6391	7136	6749	2545	2.323462	6529.5	N
SLF-4	Gastropod	D-AMS 050647	(292–297)	294.5	44.8	0.16	6450	29	−254	151	6810	7178	6631	7345	6999	3445	3.6	6874	N
SLF-4	Gastropod	D-AMS 050648	(332–337)	334.5	44.43	0.14	6517	25	−254	151	6896	7252	6715	7411	7069	3845	5.714286	7034	N
SLF-5	Gastropod	D-AMS 050649	(15–20)	17.5	46.29	0.15	6187	26	−254	151	6509	6891	6334	7085	6707	575			N
SLF-5	Gastropod	D-AMS 050650	(80–85)	82.5	45	0.22	6414	29	−254	151	6781	7151	6592	7314	6960	1225	2.56917	6833.5	N
SLS-1	Gastropod	D-AMS 050651	(15–20)	17.5	113.19	0.26	0	0	−254	151					Modern	11,275		3480	N
SLS-1	Gastropod	D-AMS 050652	(100–105)	102.5	94.94	0.27	417	23	−254	151	1	240	1	417	175	12,125	4.857143	87.5	N
SLS-1	Gastropod	D-AMS 050653	(194–199)	196.5	74.59	0.2	2355	22	−254	151	1921	2320	1709	2533	2120	13,065	0.48329	1147.5	N
SLS-2	Gastropod	D-AMS 050654	(20–25)	22.5	81.61	0.22	1632	22	−254	151	1112	1461	932	1629	1284	7325			Y
SLS-2	Gastropod	D-AMS 050655	(95–100)	97.5	103.06	0.24	0	0	−254	151					Modern	8075			N
SLS-2	Gastropod	D-AMS 050656	(140–146)	142.5	78.92	0.19	1902	19	−254	151	1378	1743	1242	1961	1577	8525	4.095563	1430.5	N
SLS-3	Gastropod	D-AMS 050657	(35–41)	38	94.63	0.22	443	19	−254	151	30	264	1	432	189	6980			N
KKI-1	Gastropod	D-AMS 050658	(25–30)	27.5	95.48	0.24	372	20	−254	151	1	215		391	152	−725			N
KKI-1	Gastropod	D-AMS 050659	(105–110)	107.5	113.87	0.26	0	0	−254	151					Modern	75			Y
KKF-1	Gastropod	D-AMS 050660	(5–10)	7.5	105.59	0.24	0	0	−254	151					Modern	1075			N
KKF-1	Gastropod	D-AMS 050661	(65–71)	68	95.06	0.25	407	21	−254	151	1	234	1	411	170	1680	3.558824		N
KKF-2	Gastropod	D-AMS 050662	(5–10)	7.5	94.61	0.34	445	29	−254	151	13	266	1	435	191	1375		85	N
KKF-2	Bivalve	D-AMS 050663	(75–80)	77.5	50.59	0.19	5474	30	−254	151	5745	6118	5583	6276	5935	2075	0.121866	3063	N
KKF-3	Gastropod	D-AMS 050664	(10–15)	12.5	95.81	0.24	344	20	−254	151					Modern	1325			N
KKF-3	Gastropod	D-AMS 050665	(110–115)	112.5	50.01	0.19	5566	31	−254	151	5865	6222	5663	6378	6033	2325	0.165755	3016.5	N
KKF-3	Gastropod	D-AMS 050666	(201–206)	203.5	48.83	0.19	5758	31	−254	151	6043	6410	5887	6607	6236	3235	4.482759	6134.5	N
KKF-3	Gastropod	D-AMS 050667	(246–251)	248.5	48.06	0.17	5886	28	−254	151	6198	6556	6002	6735	6379	3685	3.146853	6307.5	N
KKF-4	Gastropod	D-AMS 050668	(15–20)	17.5	92.92	0.24	590	21	−254	151	146	451	1	531	299	1575			N
KKF-4	Gastropod	D-AMS 050669	(105–110)	107.5	43.74	0.17	6643	31	−254	151	7035	7382	6839	7523	7200	2475	0.130416	3749.5	N
KKS-1	Gastropod	D-AMS 050670	(15–20)	17.5	110.61	0.27	0	0	−254	151					Modern	10,075			N
KKS-1	Bivalve	D-AMS 050671	(105–110)	107.5	91.01	0.22	757	19	−254	151	300	591	121	727	444	10,975	2.027027	222	N
KKS-2	Gastropod	D-AMS 050672	(20–25)	22.5	105.68	0.26	0	0	−254	151					Modern	7425	2.224138	145	N
KKS-2	Gastropod	D-AMS 050673	(85–89)	87	93.05	0.33	579	28	−254	151	138	444	1	523	290	8070			N
KKS-3	Bivalve	D-AMS 050674	(10–15)	12.5	105.05	0.23	0	0	−254	151					Modern	6125			N
KKS-3	Gastropod	D-AMS 050675	(65–70)	67.5	94.71	0.24	437	20	−254	151	30	256	1	428	186	6675	2.956989	93	N
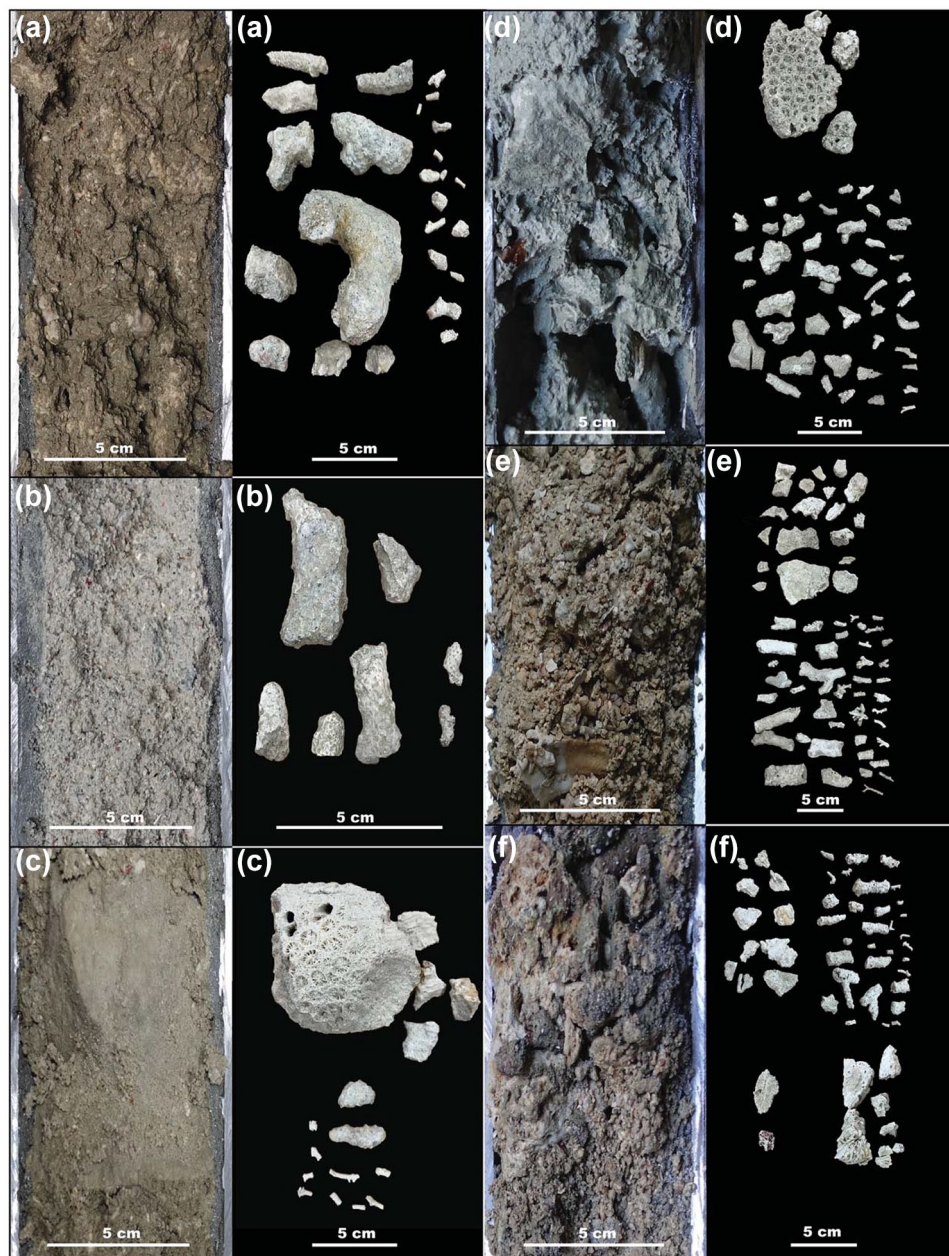
Figure 4. Core and >2 mm size fraction corals for each facies described in this studies cores. (a) Branching dominant rudstone facies. (b) Branching dominant floatstone facies. (c) Massive dominant rudstone facies. (d) Branching/massive rudstone facies. (e) Branching/Foliose rudstone facies. (f) Mixed morphology rudstone facies.

and in many cases the massive coral takes up the majority (if not all) of the coring tube. The massive/branching rudstone facies (Figure 4d) has a mixture of branching and massive corals dominating, often there are pieces of a massive coral within the subsample (most frequently pieces of a massive *Galaxea* colony). Figure 4e shows the branching/foliose rudstone facies comprised of a majority (but relatively equal amounts) of branching and foliose corals dominating the sub sample. Finally, Figure 4f, is the mixed rudstone facies, a clast supported facies of all three major morphologies mixed together. The majority of cores returned a rudstone, sand matrix-infilled facies (Figures 4 and 5). These facies frameworks were dominantly branching coral (Figures 4 and 5). However, there also were 4 and 3 reef flat cores from Samalona and Kudingareng Keke respectively, with a facies of massive dominantly or massive mixed rudstone facies appearing before and up to 5500 YBP. Reef slope cores tended to have more massive and foliose corals, with Kudingareng Keke slope cores having dominant foliose/massive/branching coral mixes. Samalona slope cores showed more dominantly branching facies,

but with a higher occurrence of foliose and massive corals than seen on the Samalona flat cores.

Almost all reef cores showed a general grain size fining down-core trend (mean grain size). Grain size is very to extremely poorly sorted across all cores (Figure 6, Supplemental Figure 1). Reef flat cores went from coarse sand mean grain size at the top of the core to fine sand at the bottom, with the transition beginning between 0.5 and 1.5 m downcore (Figure 6, Supplemental Figures 2 and 3). As the mean grain size reduces toward medium to fine sand, with finer sand more likely at the bottom of the longer reef flat cores, the remaining grain size is increasingly filled by silt and mud sized particles. This is accompanied by a visual shift in color from a brown coarse sand matrix to an increasingly gray lime mud matrix. Reef slope cores (Supplemental Figures 1 and 4) on Samalona show a very slight fining downward sequence, from coarse to medium sand. On Kudingareng Keke slope, there is a much more pronounced fining downward sequence from very coarse/coarse sand to fine sand. The Kudingareng Keke island core is dominantly sand matrix, with most coral fragments of
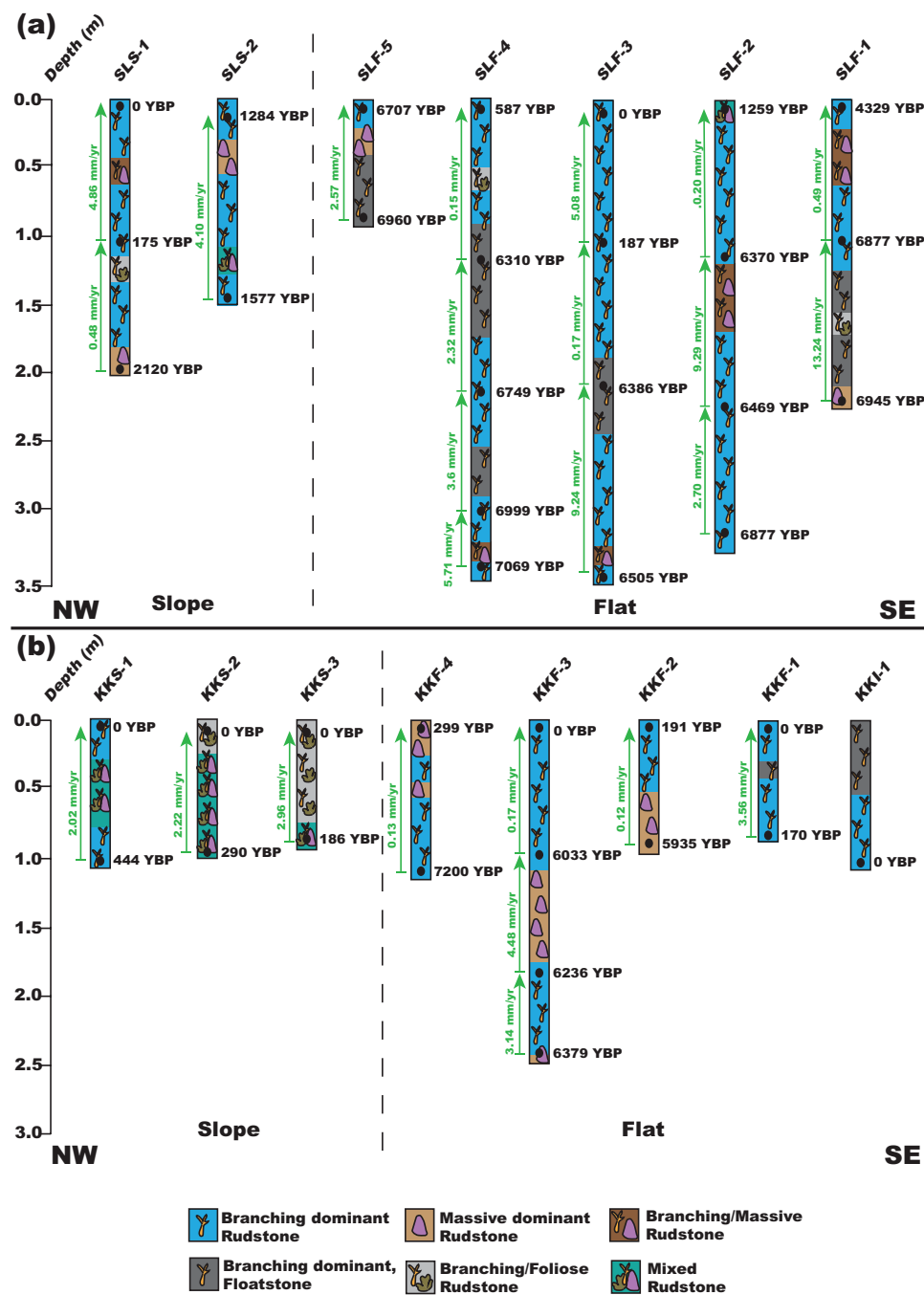
Figure 5. (a) Mean accretion rates (green/arrows), calYBP ^{14}C dates (black), and facies of Samalona cores. Core names are at the top. (b) Mean accretion rates (green/arrows), calYBP ^{14}C dates (black), and facies of Kudingareng Keke cores. Core names are at the bottom.
Note. Please refer to the online version of the article to view this figure in color.

>2 mm being eroded when present. This creates an almost entirely matrix dominant floatstone facies with minimal reef framework. Coral is minimal in the >2 mm fraction of this core, and the grain size shows poor sorting and does not follow the downward fining sequence we see in other cores from this study.

Radiometric dates

We returned 45 radiocarbon dates, of which four represented age reversals, three on Samalona and one from the Kudingareng Keke island core (Figures 2, 3, and 5, Table 2). These reef flat age reversals are less than 100 years and are close to the 2σ range of the ^{14}C dates, and therefore may not be a true age reversal. Still, all age

reversals were excluded from calculation of MAR for more accurate comparisons both between islands and to global and regional MAR (Hynes et al., 2024). On both reef flats the majority of cores are Modern – 1300 YBP at the core top. The only exceptions to this are the Samalona cores taken near the island and the reef crest (4329 and 6707 YBP respectively). Moving downcore by 1 m then yields an age between 5900 and 7200 YBP on all flat cores except SLF-3 (mid reef flat), where this transition occurs approximately 2 m downcore. Reef slope cores are much younger, with all but one being modern at the top and reaching up to 2120 YBP at the bottom. Paleo reef depth (PRD) was plotted against the calibrated Ages (YBP) as seen in Figure 7, and compared and contrasted with the other core study from Spermonde (Kappelmann et al., 2023).
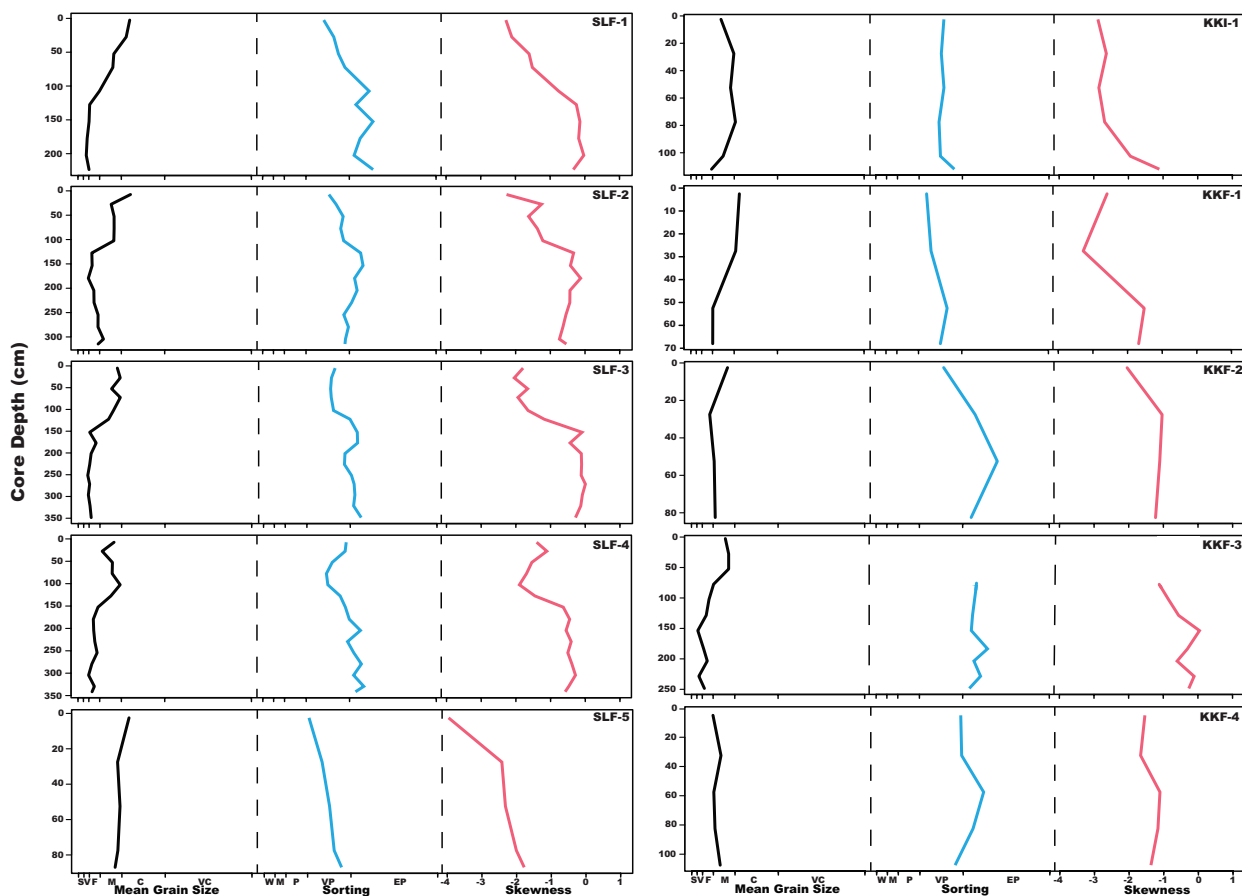
Figure 6. Mean Grain Size, Sorting, and Skewness Curves for Samalona and Kudingareng Keke reef flat cores. Core name is on the top right of each set of curves, Samalona cores on the left, Kuginagreng Keke on the right. . For Mean Grain Size, S is silt/clay, V is very fine sand, F is fine sand, M is medium sand, C is coarse sand, VC is very coarse sand. For Sorting, W is well sorted, M is moderately sorted, P is poorly sorted, VP is very poorly sorted, EP is extremely poorly sorted.

Accretion rates

Reef flat accretion can be broken up into two distinct periods, Early to Mid-Holocene (approximately 7200–5500 YBP) and Mid to Late Holocene (5500 YBP to Modern). On Samalona in the Early Holocene we found accretion rates ranging from 2.32 to 13.25 mm/yr with a mean of 6.08 mm/yr. After this point accretion slows down drastically to an average of 1.20 mm/yr (0.15–5.08 mm/yr). Similarly, on Kudingareng Keke we found accretion rates ranging from 3.14 to 4.48 mm/yr with a mean of 3.81 mm/yr in the Early Holocene. The Late-Holocene on Kudingareng Keke saw MAR ranging from 0.12 to 3.56 mm/yr, with a mean of 1.00 mm/yr, mirroring the MAR slowdown observed on Samalona. Reef slopes only cover the last 2100 years, and therefore can only tell us about MAR from this period. Here we observed a MAR ranging from 0.48 to 4.86 mm/yr with a mean of 2.77 mm/yr. These rates, while lower than Early Holocene reef flat accretion, are still higher than modern accretion on the flat.

Sea level and paleo reef depth

Our reconstructed PRD are plotted relative to the Coastal West Pacific (Lambeck et al., 2014) in Supplemental Figure 5. We distinguish two phases: (1) a rapid increase in sea level from the Last Glacial Maximum (LGM) into the Mid-Holocene (Supplemental Figure 5). In this phase all reefs were rapidly accreting to follow sea level rise up to approximately 5500 YBP, a sea level highstand in the Middle Holocene, followed by a maximum 2 m sea level drop. Accretion rates dropped on the reef flat, but remained higher on the reef slope. It is only in the last few decades that sea level has started to rise again (Walker et al., 2021), but this is not visible in Supplemental Figure 5 due to ¹⁴C dating limitations.

Discussion

To examine reef platform formation and island growth in the Spermonde Archipelago (SW Sulawesi, Indonesia), reef cores were examined for geologic and geomorphologic factors. We built a robust geochronologic framework by integrating 45 radiocarbon dates from 16 cores, and we managed to reconstruct the past 7200 years of reef development. We calculated the mean accretion rates during this time interval for two islands, Samalona positioned in the Mid-Shelf, and Kudingareng Keke from the Outer Shelf. These are roughly similarly sized and shaped islands that are subject to different environmental conditions and have different coral cover patterns in the present day, but seemingly formed under similar circumstances in the Early to Mid-Holocene. It was found that both islands have similar age to depth ranges (Figures 2, 3, and 5) and accretion rates from both reef flat and reef slope cores. In addition, they have similar sedimentary facies, dominantly branching rudstone, on the flats, with massive and foliose dominant facies more commonly seen prior to 5500 YBP. The grain size regimes also show similar patterns, and therefore geomorphological processes for both islands are subject to the same controlling factors, albeit with minor local differences. Accretion rates are faster approaching the Mid-Holocene (over 6 mm/yr) but slow significantly to just over 1 mm/yr toward the present day reflecting a lack of accommodation space due to declining sea level. Based on these observations we discuss the geomorphological development of these islands in relation to environmental conditions. We do this by discussing two phases in reef development, the first during the Early to Mid-Holocene sea-level rise, the second during the Mid- to Late-Holocene sea-level drop. Finally, we integrate these data into a model of reef development of sand cay reefs.
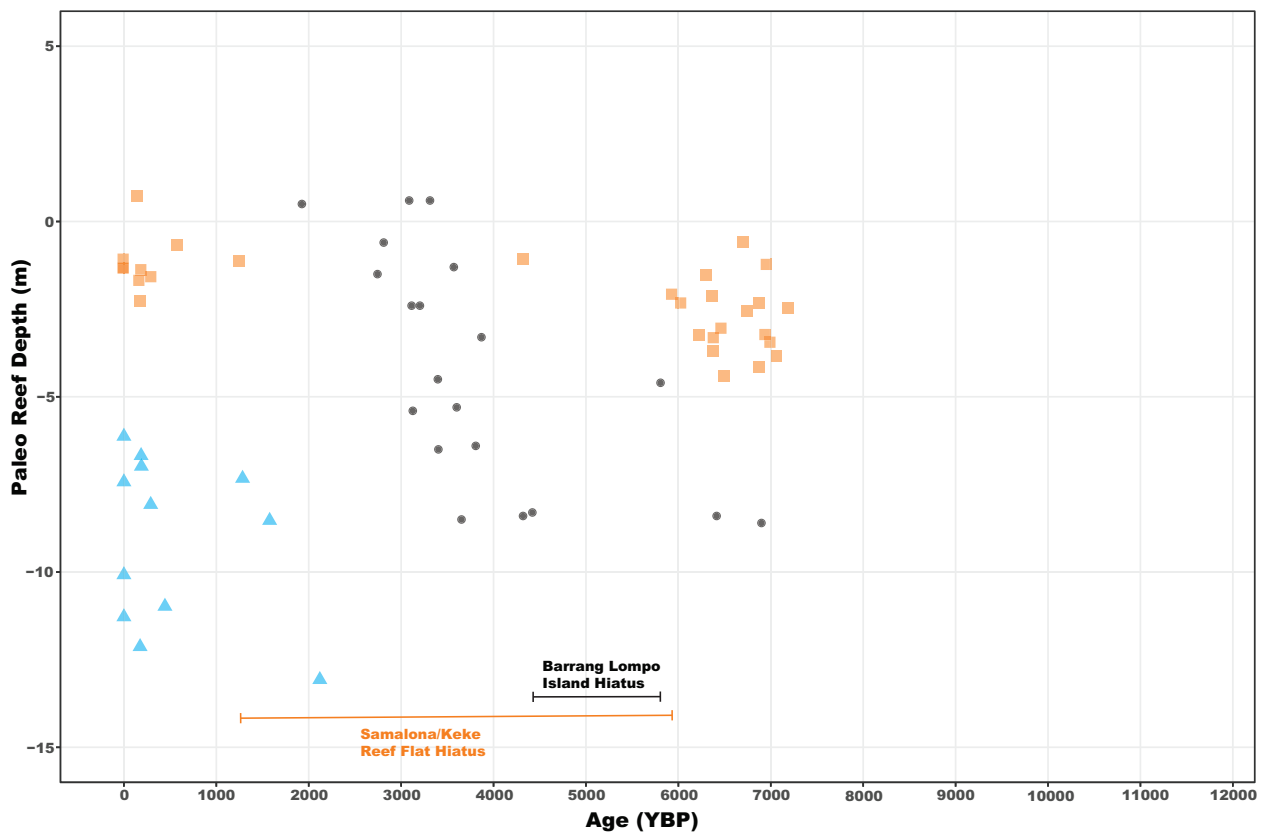
Figure 7. Paleo reef depth (core depth + water depth) versus age (YBP) plot. Orange squares are the reef flat samples and blue triangles are the reef slope samples from this study. Black dots are from Kappelmann et al. (2023) from Barang Lompo an inhabited island in the Spermonde Archipelago.

Note. Please refer to the online version of the article to view this figure in color.

Early to Mid-Holocene reef flat development (7200–5500 YBP)

While the exact point of reef initiation could not be determined due to the cores not recovering Pleistocene basement, it is likely that the oldest ages are close to point of reef imitation as the shallow depths of the mid to inner shelf of Spermonde (Kudingareng Keke and Samalona respectively) were flooded by 9000 YBP (Mann et al., 2016, 2019). Core data collected here from both islands demonstrate that the early Holocene started with reefs growing in deeper water conditions. In two reef flat cores from each island we observe a transition from a massive/foliose coral dominated rudstone facies to a branching coral dominated facies, which we interpret here as a shallowing trend. However, it cannot be ruled out that part of this trend is the result of lateral variation in facies (Webster and Davies, 2003). This period coincides with the final stages of sea level rise as the result of deglaciation following the Last Glacial Maximum (LGM) (Bender et al., 2020; Kappelmann et al., 2023; Mann et al., 2016, 2019). Both reef complexes are primarily accreting to fill the accommodation space being created by sea level rise (Dechnik et al., 2017; Hubbard et al., 1986; Twiggs and Collins, 2010). Rates of accretion have a mean of 3.81 and 6.08 mm/yr on Kudingareng Keke and Samalona respectively, which fall well within the range of the global average of accretion rates during this period (Hynes et al., 2024). As a way to keep-up with increased accommodation space, the reef shifts to a dominant branching coral rudstone facies. (Hubbard, 2009). This facies becomes the norm toward the Mid-Holocene on both reef flats.

The reef crest likely reached maximum accommodation space (1–2 m maximum water depth) early within this period, as seen by core SLF-5 where the top and bottom are between 7000 and 6000 YBP. As the reef likely become more rugose and complex, the sediment influx by both erosion of corals/rubble and input from extrinsic sources built up from the Western margin (the crest) toward the leeward side, especially during the wet season (Janßen et al., 2017). A true crest never developed on the leeward side, and to this day exists more as a gentle slope on both islands. By the end of this period, the island itself is already forming on the eastern half of the platform, toward the leeward margin. The reef flat approached sea level by 5500 YBP (sea level highstand), and is formed mostly of carbonate sediments derived from local carbonate production, subsequent reef bioerosion, and transport of sediments across the reef flat.

Mid holocene hiatus and Late-Holocene reef flat development (5500 YBP–present)

From the Mid-Holocene, where regional sea level rise not only slows, but actually begins to decline by up to 1 m (Mann et al., 2016, 2019), reefs here shifted from an accretion phase to a windward progradation/leeward accumulation (Dechnik et al., 2015, 2017; Hubbard, 2009; Twiggs and Collins, 2010). In fact, this decrease in sea level likely also contributed to the changing reef flat morphology, as well as to the diminishing amount of accommodation space (Harris et al., 2015). The facies across the reef flats of both islands show that branching corals are still dominant, though accretion rates have slowed significantly to about 1 mm/yr. This is a MAR that is low, even for global trends during this reef accretion hiatus period (Hynes et al., 2024). During this time, global MAR slows to a mean of 5 mm/yr (or less in some regions), while in the Coastal West Pacific it drops to below 5 mm/yr from 6000 to 3000 YBP. This pattern is present globally, and has been interpreted as a Mid-Holocene Reef Hiatus (Dechnik et al., 2017; Grossman and Fletcher, 2004; Leonard et al., 2020; Toth et al., 2015). A global reef hiatus could be explained by the change in sea level regime, where most regions see a slowdown of sea level
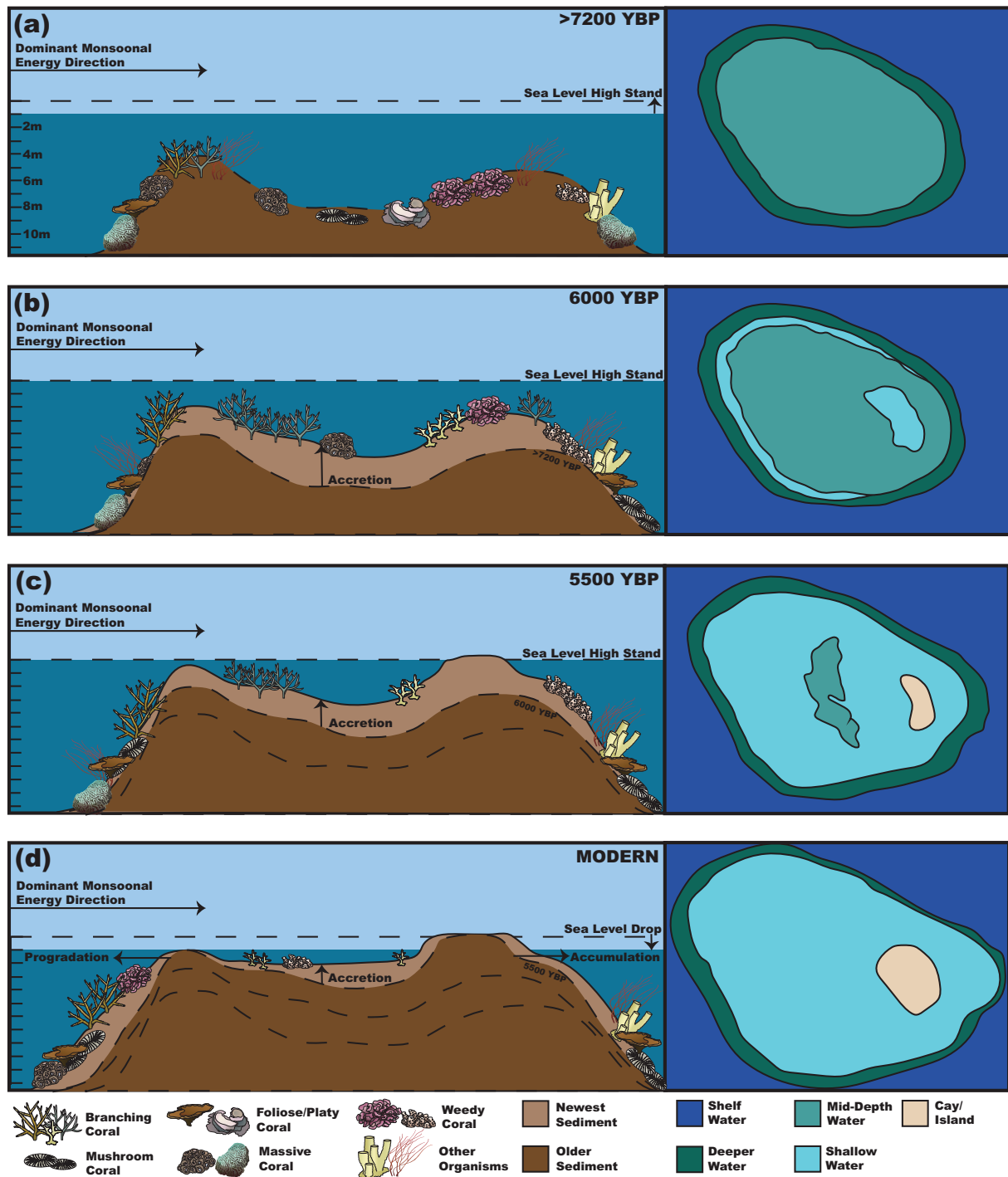
Figure 8. Model of island platform development for the Spermonde Archipelago. (a) Initial reef phase captured at the bottom of the cores. (b) Rapid vertical accretion phase to keep up with the last of the sea level rise regime coming out of the LGM. (c) A sand cay has formed and begun to emerge on the Eastern edge of the reef. (d) Modern day, where with sea level drop the island has grown and expanded due to accumulation of sediment on the island, and the Western margin is prograding. Organism symbols are from Integration and Application Network (IAN) at UCMES (ian.umces.edu/media-library).

rise, often shifting toward a decline in the Mid- to Late-Holocene (Hynes et al., 2024; Khan et al., 2019; Lambeck et al., 2014). Therefore, accretion for Spermonde slowed down well below the global and regional averages. This is due to the fact that by 6000 YBP, with sea level fall there is minimal accommodation space left on the outer margins of the reef flat, with only the middle part of the flat infilling with sediment (Kappelmann et al., 2023; Mann et al., 2019). Sediment transport is still in the seaward to leeward direction, but as we move ever closer to the present there is less room for sediment to be trapped on the flat, and therefore tending to move toward building up the island, and down the leeward slope (Janßen et al., 2017; Kench and Mann, 2017).

By the last few millennia, the island on both platforms has fully formed and is above sea level, continually growing (albeit slowly) due to sediment build up and sea level decline. Samalona island likely fully emerged after the drop in sea level post 5500 YBP (SLF-1 at the top of the core is 4329 YBP, in front of the island). On Kudingareng Keke, we see that the island possibly emerged more recently than Samalona, but certainly the emergence of the sand cay here was also aided by the decline in sea level. The reef flat has all but infilled, and there is stability on the platform of sediment generation, as well as coral growth on the surrounding reef slopes. The age reversal on Kudingareng Keke island is likely due to constant reworking of this part of the island

by seasonal changes and sedimentation through erosion and transport (Kench and Mann, 2017). Coral coverage has declined on the flats over the last few decades (Best et al., 1989; Moll and Borel-Best, 1984; Yasir Haya and Fujii, 2017) as accommodation space is less than a meter at points, and between 0 and 1.5 m (MSL) on the majority of the flat. As water depth decreased, there was little room for vertical accretion and therefore coral growth. This decline is also due to the high anthropogenic influence of the population through nutrification and runoff, destructive fishing practices and increased tourism (Yasir Haya and Fujii, 2017). With the crest, flat, and island all being near, at or above sea level, the platforms then begin to prograde on the seaward (Western) slope, and accumulate on the island and eastern edge.

Late-Holocene to recent reef slope development

In the reef slope cores we observed radiometric ages up to 2120 years old on both islands. Samalona slope cores SLS-[1-2] have the oldest dates compared to Kudingareng Keke, but these cores are also up to 1 m longer, and therefore capture more of the reef's history. These maximum ages are younger than those seen in the reef flat cores, and overlap with the last phase of reef flat development. These observations match a shift to the slope prograding outwards to the seaward slope where there is maximum accommodation space, and the eastern edge now sees increased accumulation, especially on the island (Gischler et al., 2019; Smithers et al., 2006). Mean accretion rates on the slope show continuous sedimentation, and are faster than the reef flat on both islands over the last 2000 years at an average of 2.77 mm/yr (although this is still significantly lower than global and regional averages for this time period). This is to be expected due to there being plentiful accommodation space and higher levels of carbonate production on the reef slope, which matches observations seen elsewhere (Bender et al., 2020; Gischler and Hudson, 2019; Hubbard, 2009; Mann et al., 2019).

Model of island formation

We have summarized these findings in a model of reef formation in the Spermonde (Figure 8). These reefs initiated on top of earlier Cenozoic carbonates, with a mixed coral community consisting of foliose and massive growth forms. Until 5500 YBP, the reefs predominantly accreted to keep up with sea level change. This is documented in our reef cores by comparable accretion rates across the entire reef flat. While Kudingareng Keke and Samalona are relatively small islands, in larger reefs, accretion rates might be more variable resulting in an uneven top of the reef. This is different from the bucket infill model (Harris et al., 2015; O'Leary and Perry, 2010), during which in the initial phase accretion rates are higher around the reef edges, and these are subsequently filled in with sediment once the reef top reaches sea level. In this model, one would expect the oldest ages to be found at the reef edge, and younger sediments in the central part of the reef flat. The slowdown and cessation of sea level rise resulted in a reduction in accommodation space, and an accompanying strong reduction in accretion rates. A large part of this period is associated with an apparent hiatus in reef growth on the reef flat from 6000 to 2000 YBP, irregular morphology, and is driven by limited accommodation space and likely not by environmental conditions (although here we lack sediments of sufficient age on the reef slope to test this). This hiatus, in Spermonde, is also seen globally as a period of minimal reef accretion (Dechnik et al., 2017; Leonard et al., 2020; Perry and Smithers, 2011; Toth et al., 2012). The reef flat is capped by approximately 1 m of post-hiatus sediments. These have predominantly a branching rudstone facies and a coarser grain size, which might indicate a period of continued carbonate production and coral growth on the reef flat and sediment transport across the reef flat resulting in island formation. At the same time, accretion rates on the reef slope are faster than the flat during the Late-Holocene. This represents a shift from accreting to progradation on the western slope/flat, and accumulation on the island and the eastern slope.

Due to Spermonde being tectonically stable (Prasetya et al., 2001) it is clear that sea level is one of the major driving extrinsic factors of patch reef accretion and island formation (Bender et al., 2020; Janßen et al., 2017; Mann et al., 2019). This is seen in the shift from a more mixed coral rudstone facies, to dominantly branching corals, as well as a major reduction in accretion rates coinciding with sea level in the region hitting a Mid-Holocene high-stand and then declining slightly. Traditional models of sand cay formations on (patch) reef complexes include the lagoonal (or bucket) infill model (Harris et al., 2015; O'Leary and Perry, 2010). Another core study from the Spermonde archipelago suggests that a different island, Barrang Lompo, had seen a lagoonal infill from the Mid-Holocene to present where the island now exists (Kappelmann et al., 2023). In this study they also found a hiatus in reef growth from 5700 to 4200 YBP, which is both shorter in duration and occurs earlier than the Mid-Holocene reef growth hiatus observed in other regions and on a global scale (Dechnik et al., 2017; Hynes et al., 2024; Toth et al., 2012). However, this suite of cores was taken from the island itself, and therefore offers no direct insight to reef flat and slope formation. Further, Barrang Lompo is an irregular shaped patch reef complex (possibly formed by the junction of two smaller patch reefs), unlike the more uniformly formed islands such as Samalona and Kudingareng Keke.

In the cores taken in this study from Samalona and Kudingareng Keke, there is no clear evidence of a lagoon on the eastern portion of the island/leeward margin of the platform, though no core was taken on the eastward margin. Further, the reef flat growth hiatus occurs from approximately 6000–1500 YBP, which is more in line with what is observed globally (Hynes et al., 2024), and occurs during a period of consistent declining sea level in the region. What is likely represented by this change in facies and accompanying reef accretion hiatus is due to sea level regimes and the shift from vertical accretion to progradation/accumulation on the patch reef margins (Janßen et al., 2017; Kench and Mann, 2017). In fact, island formation here is more akin to what is seen in the Capricorn bunker group of the Great Barrier Reef (Dechnik et al., 2015, 2016, 2017). This is shown by the reef margins forming first (Figure 8a), followed by the flat accreting vertically from 7200 to 5500 YBP (Figure 8b and c) and subsequently a Mid-Holocene growth hiatus (due to declining sea level). After 5500 YBP the sand cays become sub-aerially exposed, especially after the sea level drop of 0.5–1 m (Figure 8c and d), and reef accretion is now mostly restricted to the slopes, especially on the seaward margin in a progradation phase (Figure 8d). The island and eastern margin see an accumulation of reef sediment transported across the flat from the production zone of the slope and crest. However it should be noted that in Spermonde, subsidence has had minimal impact on reef formation throughout the Holocene, as opposed to the Capricorn bunker group and the Great Barrier Reef as a whole (Crameri and Lithgow-Bertelloni, 2018).

As many islands in the Spermonde Archipelago are heavily populated today and the coral reef complexes surrounding them are a significant economic source for these people, it is pertinent that we understand if these islands can still generate enough sediment and grow at rates fast enough to combat future erosion as sea level regimes change. We show here that in the past, these islands initiated under rapid sea level rise and were able to grow at rates needed to survive and not become "drowned" reefs (Hubbard, 2009). Finally, as there was previously a lack of data on Holocene reef accretion in the Coral Triangle, we can use the MAR calculated here to understand the region's history, as well as future forecast models of reef accretion in South Sulawesi, and the Coral Triangle.

Conclusion

The islands in the Spermonde Archipelago were heavily influenced by rapid Relative Sea Level rise (RSL) during their formation and subsequent accumulation. During the Early to Mid-Holocene period, it was found that Mean Accretion Rates (MAR) were rapid as reefs were in a catch-up/keep-up phase of accretion. As RSL plateaued in the Mid-Holocene and then declined moving toward the Modern, MAR slowed significantly, especially on the reef flat, as these reefs filled up the remaining accommodation space. This then led to a progradation phase on the slope which is still active today, as reef slope accretion is still within normal ranges. Therefore, island formation did not happen by lagoonal infill (or bucket infill) model, but by continuous accretion controlled extrinsically by sea level.

This shows that islands in the area were able to keep up with varying levels of sea level rise in the past, including the fast rates seen in the Early to Mid-Holocene (Hynes et al., 2024). As significant increases in sea level are expected to occur in the coming decades and centuries, this demonstrates that reefs in the Spermonde Archipelago have the ability to accrete at rates necessary to avoid drowning. However, this assumes that they do not face high levels of additional stressors other than sea level rise (such as thermal stress/bleaching, excess nutrification/eutrophication, and overfishing). As only three sets of core studies for the Spermonde archipelago, including this suite of cores (Kappelmann et al., 2023, 2024), and only one additional core study from the Coral Triangle (Grobe et al., 1985) exist, it would be beneficial to obtain more records of Holocene reef accretion within this region, which is the area of highest coral diversity and growth globally.

Author contribution(s)

Michael G. Hynes: Conceptualization; Data curation; Formal analysis; Investigation; Methodology; Supervision; Validation; Visualization; Writing – original draft; Writing – review & editing.
Halwi Masdar: Investigation; Methodology; Resources; Writing – review & editing.
Dedi Parenden: Data curation; Investigation; Writing – review & editing.
Nicole J. de Voogd: Conceptualization; Funding acquisition; Methodology; Supervision; Validation; Writing – review & editing.
Jan-Berend W. Stuut: Investigation; Methodology; Writing – review & editing.
Jamaluddin Jompa: Conceptualization; Funding acquisition; Resources; Writing – review & editing.
Jody M. Webster: Data curation; Methodology; Validation; Writing – review & editing.
Willem Renema: Conceptualization; Funding acquisition; Investigation; Methodology; Project administration; Supervision; Validation; Writing – review & editing.

ORCID iDs

Michael G Hynes https://orcid.org/0000-0001-6154-5598
Dedi Parenden https://orcid.org/0009-0006-4974-6745
Nicole J de Voogd https://orcid.org/0000-0002-7985-5604

Supplemental material

Supplemental material for this article is available online.

References

Ballesteros LV, Matthews JL and Hoeksema BW (2018) Pollution and coral damage caused by derelict fishing gear on coral reefs around koh Tao, Gulf of Thailand. *Marine Pollution Bulletin* 135: 1107–1116.

Bejarano S, Pardede S, Campbell SJ et al. (2019) Herbivorous fish rise as a destructive fishing practice falls in an Indonesian marine national park. *Ecological Applications* 29(8): e01981.

Bender M, Mann T, Stocchi P et al. (2020) Late holocene (0-6 ka) sea-level changes in the Makassar Strait, Indonesia. *Climate of the Past* 16(4): 1187–1205.

Best MB, Hoeksema BW, Moka W et al. (1989) Recent scleractinian coral species collected during the Snellius-ii expedition in eastern Indonesia. *Netherlands Journal of Sea Research* 23(2): 107–115.

Boggs S Jr. (2012) *Principles of Sedimentology and Stratigraphy*. Upper Saddle River, NJ: Pearson Education Ltd.

Crameri F and Lithgow-Bertelloni C (2018) Abrupt upper-plate tilting during slab-transition-zone collision. *Tectonophysics* 746: 199–211.

Cramer KL, O'Dea A, Clark TR et al. (2017) Prehistorical and historical declines in Caribbean coral reef accretion rates driven by loss of parrotfish. *Nature Communications* 8: 14160.

Dechnik B, Bastos AC, Vieira LS et al. (2019) Holocene reef growth in the tropical southwestern Atlantic: Evidence for sea level and climate instability. *Quaternary Science Reviews* 218: 365–377.

Dechnik B, Webster JM, Davies PJ et al. (2015) Holocene "turn-on" and evolution of the Southern Great Barrier Reef: Revisiting reef cores from the Capricorn Bunker Group. *Marine Geology* 363: 174–190.

Dechnik B, Webster JM, Nothdurft L et al. (2016) Influence of hydrodynamic energy on holocene reef flat accretion, Great Barrier Reef. *Quaternary Research* 85(1): 44–53.

Dechnik B, Webster JM, Webb GE et al. (2017) Successive phases of holocene reef flat development: Evidence from the mid- to outer Great Barrier Reef. *Palaeogeography Palaeoclimatology Palaeoecology* 466: 221–230.

de Klerk LG (1983) Zeespiegels, riffen en kustvlakten in zuidwest Sulawesi, Indonesie| een morfogenetisch-bodemkundige studie (Sea levels, coral reefs and coastal plains in southwest Sulawesi, Indonesia). *Utrechtse Geografische Studies Utrecht* (27): 172.

Girard EB, Estradivari, Ferse S et al. (2022) Dynamics of large benthic foraminiferal assemblages: A tool to foreshadow

reef degradation? *Science of the Total Environment* 811: 151396.

Gischler E (2008) Accretion patterns in holocene tropical coral reefs: Do massive coral reefs in deeper water with slowly growing corals accrete faster than shallower branched coral reefs with rapidly growing corals? *International Journal of Earth Sciences* 97(4): 851–859.

Gischler E and Hudson JH (2019) Holocene tropical reef accretion and lagoon sedimentation: A quantitative approach to the influence of sea-level rise, climate and subsidence (Belize, Maldives, French Polynesia). *Depositional Record* 5(3): 515–539.

Gischler E, Hudson JH, Humblet M et al. (2019) Holocene and pleistocene fringing reef growth and the role of accommodation space and exposure to waves and currents (Bora Bora, Society Islands, French Polynesia). *Sedimentology* 66(1): 305–328.

Grobe H, Willkom H and Wefer G (1985) Internal structure and origin of the double reefs of north Bohol and the Olango Reef Flat (philippines). *Philippine Scientist* 22(1): 83–94.

Grossman EE and Fletcher CH (2004) Holocene reef development where wave energy reduces accommodaton space, Kailua Bay, Windward Oahu, Hawaii, USA. *Journal of Sedimentary Research* 74(1): 49–63.

Hammerman NM, Roff G, Rodriguez-Ramirez A et al. (2022) Reef accumulation is decoupled from recent degradation in the central and southern red Sea. *Science of the Total Environment* 809: 151176.

Harris DL, Webster JM, Vila-Concejo A et al. (2015) Late holocene sea-level fall and turn-off of reef flat carbonate production: Rethinking bucket fill and coral reef growth models. *Geology* 43(2): 175–178.

Heaton TJ, Köhler P, Butzin M et al. (2020) Marine20 the marine radiocarbon age calibration curve (0-55,0000 BP). *Radiocarbon* 62(4): 779–820.

Hoegh-Guldberg O, Pendleton L and Kaup A (2019) People and the changing nature of coral reefs. *Regional Studies in Marine Science* 30: 100699.

Hoeksema BW (2007) Delineation of the indo-Malayan centre of maximum marine biodiversity: The coral triangle. In: *Biogeography, Time, and Place: Distributions, Barriers, and Islands*. Dordrecht, Springer Netherlands, pp.117–178.

Hubbard DK (2009) Depth-related and species-related patterns of Holocene reef accretion in the Caribbean and western Atlantic: A critical assessment of existing models. In: Swart PK, Eberli GP and McKenzie J (eds) *Perspectives in Carbonate Geology: A Tribute to the Career of Robert Nathan Ginsburg*, vol. 41. Chichester: Wiley, pp.1–18.

Hubbard DK, Burke RB and Gill IP (1986) Styles of reef accretion along a steep, shelf-edge reef, St. Croix, U.S. Virgin Islands. *Journal of Sedimentary Petrology* 56(6): 848–861.

Hynes MG, O'Dea A, Webster JM et al. (2024) RADReef: A global holocene reef rate of accretion dataset. *Scientific Data* 11(1): 398.

Janßen A, Wizemann A, Klicpera A et al. (2017) Sediment composition and facies of coral reef islands in the Spermonde Archipelago, Indonesia. *Frontiers in Marine Science* 4: 144.

Januchowski-Hartley FA, Graham NAJ, Wilson SK et al. (2017) Drivers and predictions of coral reef carbonate budget trajectories. *Proceedings of The Royal Society B Biological Sciences* 284(1847): 20162533.

Kappelmann Y, Sengupta M, Mann T et al. (2024) Island accretion within a degraded reef ecosystem suggests adaptability to ecological transitions. *Sedimentary Geology* 468: 106675.

Kappelmann Y, Westphal H, Kneer D et al. (2023) Fluctuating sea-level and reversing monsoon winds drive holocene lagoon infill in Southeast Asia. *Scientific Reports* 13(1): 5042.

Kench PS, Beetham EP, Turner T et al. (2022) Sustained coral reef growth in the critical wave dissipation zone of a Maldivian atoll. *Communications Earth & Environment* 3(1): 9.

Kench PS and Mann T (2017) Reef Island Evolution and Dynamics: Insights from the Indian and Pacific Oceans and perspectives for the Spermonde Archipelago. *Frontiers in Marine Science* 4: 145.

Khan NS, Horton BP, Engelhart S et al. (2019) Inception of a global atlas of sea levels since the Last Glacial Maximum. *Quaternary Science Reviews* 220: 359–371.

Kidwell SM (1997) Time-averaging in the marine fossil record: Overview of strategies and uncertainties. *Geobios* 30(7): 977–995.

Kidwell SM (2013) Time-averaging and fidelity of modern death assemblages: building a taphonomic foundation for conservation palaeobiology. *Palaeontology* 56(3): 487–522.

Lambeck K, Rouby H, Purcell A et al. (2014) Sea level and global ice volumes from the Last Glacial Maximum to the holocene. *Proceedings of the National Academy of Sciences of the United States of America* 111(43): 15296–15303.

Lane DJW and Hoeksema BW (2016) Mesophotic mushroom coral records at Brunei Darussalam support westward extension of the Coral Triangle to the South China Sea waters of northwest Borneo. *Raffles Bulletin of Zoology* 64: 204–212.

Lange ID, Perry CT and Alvarez-Filip L (2020) Carbonate budgets as indicators of functional reef "health": A critical review of data underpinning census-based methods and current knowledge gaps. *Ecological Indicators* 110: 105857.

Leonard ND, Lepore ML, Zhao JX et al. (2020) Re-evaluating mid-holocene reef "turn-off" on the inshore Southern Great Barrier Reef. *Quaternary Science Reviews* 244: 106518.

Łukowiak M, Cramer KL, Madzia D et al. (2018) Historical change in a Caribbean reef sponge community and long-term loss of sponge predators. *Marine Ecology Progress Series* 601: 127–137.

Macintyre IG and Glynn PW (1976) Evolution of a modern Caribbean fringing reef, Galeta Point, panama. *AAPG Bulletin* 60(7): 1054–1072.

Mann T, Bender M, Lorscheid T et al. (2019) Holocene sea levels in Southeast Asia, Maldives, India and Sri Lanka: The SEAMIS database. *Quaternary Science Reviews* 219: 112–125.

Mann T, Rovere A, Schöne T et al. (2016) The magnitude of a mid-holocene sea-level highstand in the Strait of Makassar. *Geomorphology* 257: 155–163.

Moll H (1983) *Zonation and Diversity of Sclearactinia on Reefs Off SW Sulawesi, Indonesia*. Doctoral dissertation, Leiden.

Moll H and Borel-Best M (1984) New scleractinian corals (anthozoa: Scleractinia) from the Spermonde Archipelago, South Sulawesi, Indonesia. *Zoologische Mededelingen* 58(4): 47–58.

Montaggioni LF, Martin-Garin B, Salvat B et al. (2021) Coral conglomerate platforms as foundations for low-lying, reef islands in the French Polynesia (central south Pacific): New insights into the timing and mode of formation. *Marine Geology* 437: 106500.

Morgan KM, Perry CT, Arthur R et al. (2020) Projections of coral cover and habitat change on turbid reefs under future sea-level rise. *Proceedings of* T*he Royal Society B Biological Sciences* 287(1929): 20200541.

Morgan KM, Perry CT, Smithers SG et al. (2016) Transitions in coral reef accretion rates linked to intrinsic ecological shifts on turbid-zone nearshore reefs. *Geology* 44(12): 995–998.

O'Leary MJ and Perry CT (2010) Holocene reef accretion on the Rodrigues carbonate platform: An alternative to the classic "bucket-fill" model. *Geology* 38(9): 855–858.

Palmer SE, Perry CT, Smithers SG et al. (2010) Internal structure and accretionary history of a nearshore, turbid-zone coral reef: Paluma Shoals, central Great Barrier Reef, Australia. *Marine Geology* 276(1-4): 14–29.

Perry CT, Morgan KM, Lange ID et al. (2020) Bleaching-driven reef community shifts drive pulses of increased reef sediment generation. *Royal Society Open Science* 7(4): 192153.

Perry CT, Murphy GN, Graham NA et al. (2015) Remote coral reefs can sustain high growth potential and may match future sea-level trends. *Scientific Reports* 5: 18289.

Perry CT, Murphy GN, Kench PS et al. (2013) Caribbean-wide decline in carbonate production threatens coral reef growth. *Nature Communications* 4: 1402.

Perry CT and Smithers SG (2010) Evidence for the episodic "turn on" and "turn off" of turbid-zone coral reefs during the late holocene sea-level highstand. *Geology* 38(2): 119–122.

Perry CT and Smithers SG (2011) Cycles of coral reef 'turn-on', rapid growth and 'turn-off' over the past 8500 years: A context for understanding modern ecological states and trajectories. *Global Change Biology* 17(1): 76–86.

Perry CT, Smithers SG, Roche RC et al. (2011) Recurrent patterns of coral community and sediment facies development through successive phases of holocene inner-shelf reef growth and decline. *Marine Geology* 289(1–4): 60–71.

Plass-Johnson JG, Taylor MH, Husain AA et al. (2016) Non-random variability in functional composition of coral reef fish communities along an environmental gradient. *PLoS One* 11(4): e0154014.

Prasetya GS, De Lange WP and Healy TR (2001) The Makassar strait tsunamigenic region, Indonesia. *Natural Hazards* 24(3): 295–307.

Renema W, Bellwood DR, Braga JC et al. (2008) Hopping hotspots: Global shifts in marine Biodiversity. *Science* 321(5889): 654–657.

Renema W and Troelstra SR (2001) Larger foraminifera distribution on a mesotrophic carbonate shelf in SW Sulawesi (Indonesia). *Palaeogeography Palaeoclimatology Palaeoecology* 175(1–4): 125–146.

Ryan EJ, Hanmer K and Kench PS (2019) Massive corals maintain a positive carbonate budget of a Maldivian upper reef platform despite major bleaching event. *Scientific Reports* 9(1): 6515.

Smithers SG, Hopley D and Parnell KE (2006) Fringing and near-shore coral reefs of the Great Barrier Reef: Episodic holocene development and future prospects. *Journal of Coastal Research* 22(1): 175–187.

Stuiver M and Reimer PJ (1993) Extended C14 database and revised CALIB 3.0 C14 age calibration program. *Radiocarbon* 35(1): 215–230.

Stuiver M, Reimer PJ and Reimer RW (2022) Calib radiocarbon calibration 8.2 [www program].

Teichberg M, Wild C, Bednarz VN et al. (2018) Spatio-temporal patterns in coral reef communities of the Spermonde Archipelago, 2012-2014, I: Comprehensive reef monitoring of water and benthic indicators reflect changes in reef health. *Frontiers in Marine Science* 5: 33.

Toth LT, Aronson RB, Cobb KM et al. (2015) Climatic and biotic thresholds of coral-reef shutdown. *Nature Climate Change* 5(4): 369–374.

Toth LT, Aronson RB, Vollmer SV et al. (2012) ENSO drove 2500-year collapse of eastern Pacific coral reefs. *Science* 337(6090): 81–84.

Twiggs EJ and Collins LB (2010) Development and demise of a fringing coral reef during holocene environmental change, eastern Ningaloo Reef, Western Australia. *Marine Geology* 275(1–4): 20–36.

van der Windt N, van der Ent E, Ambo-Rappe R et al. (2020) Presence and genetic identity of Symbiodiniaceae in the bioeroding sponge genera Cliona and Spheciospongia (Clionaidae) in the Spermonde Archipelago (SW Sulawesi), Indonesia. *Frontiers in Ecology and Evolution* 8: 595452.

Veron JEN (1995) *Corals in Space and Time: The Biogeography and Evolution of the Scleractinia*. Ithaca: Cornell University Press.

Veron JEN (2000) *Corals of the world*, vol. 1–3. Townsville: Australian Institute of Marine Science, p. 1410.

Walker JS, Kopp RE, Shaw TA et al. (2021) Common era sea-level budgets along the US Atlantic coast. *Nature Communications* 12(1): 1841.

Webster JM and Davies PJ (2003) Coral variation in two deep drill cores: Significance for the pleistocene development of the Great Barrier Reef. *Sedimentary Geology* 159(1–2): 61–80.

Wickham H (2016) *Ggplot2: Elegant Graphics for Data Analysis*. New York, NY: Springer-Verlag.

Woodroffe CD, Samosorn B, Hua Q et al. (2007) Incremental accretion of a sandy reef island over the past 3000 years indicated by component-specific radiocarbon dating. *Geophysical Research Letters* 34(3): 1–5.

Yasir Haya LOM and Fujii M (2017) Mapping the change of coral reefs using remote sensing and in situ measurements: A case study in pangkajene and Kepulauan Regency, Spermonde Archipelago, Indonesia. *Journal of Oceanography* 73(5): 623–645.

Yusuf S, Beger M, Tassakka A et al. (2021) Cross shelf gradients of scleractinian corals in the Spermonde Islands, South Sulawesi, Indonesia. *Biodiversitas Journal of Biological Diversity* 22(3): 1415–1423.